Atomistic modeling of amorphous silicon carbide: An approximate first-principles study in constrained solution space

Raymond Atta-Fynn

Department of Physics and Astronomy, The University of Texas, Arlington, TX 76019, USA

E-mail: `attafynn@uta.edu`

Parthapratim Biswas

Department of Physics and Astronomy, The University of Southern Mississippi, Hattiesburg, MS 39406, USA

E-mail: `partha.biswas@usm.edu`

Abstract. Localized basis *ab initio* molecular dynamics simulation within the density functional framework has been used to generate realistic configurations of amorphous silicon carbide (*a*-SiC). Our approach consists of constructing a set of smart initial configurations that conform essential geometrical and structural aspects of the materials obtained from experimental data, which is subsequently driven via first-principles force-field to obtain the best solution in a reduced solution space. A combination of *a priori* information (primarily structural and topological) along with the ab-initio optimization of the total energy makes it possible to model large system size (1000 atoms) without compromising the quantum mechanical accuracy of the force-field to describe the complex bonding chemistry of Si and C. The structural, electronic and the vibrational properties of the models have been studied and compared to existing theoretical models and available data from experiments. We demonstrate that the approach is capable of producing large, realistic configurations of *a*-SiC from first-principles simulation that display excellent structural and electronic properties of *a*-SiC. Our study reveals the presence of predominant short-range order in the material originating from heteronuclear Si–C bonds with coordination defect concentration as small as 5% and the chemical disorder parameter of about 8%.

1. Introduction

Silicon carbide is a wide bandgap semiconductor having a range of applications from optoelectronic devices, gas turbines, heat exchangers to ceramic fans. The amorphous form of SiC is particularly interesting due to temperature stability of semiconducting properties making it possible to use under extreme condition in applications such

as high-temperature engines, turbines and reactors [1, 2, 3, 4, 5, 6, 7]. There have been a number of studies of amorphous SiC in recent years emphasizing mostly on the structural aspect of the material. Of particular importance is the nature of the short range order (SRO) in the material. Despite numerous experimental and theoretical studies, the exact nature of the SRO and the extent of its presence are still missing. While bonding in its various crystalline counterpart is sp^3 corresponding to heteronuclear Si–C bonds, the nature of bonding chemistry in a-SiC is far more complex and is not well understood. Different experimental probes on a-SiC often appears to suggest contradictory results: from presence of purely heteronuclear Si–C bonding to an admixture of heteronuclear Si–C (chemical order) and homonuclear Si–Si and C–C bonds (chemical disorder). Unlike silicon that conforms primarily to tetrahedral sp^3 bonding, the complex carbon chemistry permits the atom to hybridize via sp, sp^2 and sp^3 bond formation in the amorphous environment. The structure of the materials also depends on the growth conditions and the subsequent treatment of the sample. As a result, various experimental probes often provide a very different microscopic picture of the material.

In this communication we study the structural, electronic and vibrational properties of a 1000-atom model of a-SiC via ab $initio$ molecular dynamic simulation using a localized basis sets and pseudopotential density functional approach. Our emphasis is on developing an effective approach that models a sufficiently large system size without compromising the accuracy of the interaction among the atoms by focusing on the relevant part of the configuration space by using a suitable prior from experimental data. This has been achieved by generating a set of smart generic configurations and optimizing the resulting structural models in the reduced solution space of the first-principles force field. The paper is organized as follows. In Section 2, we provide a brief discussion of earlier works and the present state of knowledge of the material in amorphous state. Section 3 describes the essential idea behind our method and how to construct smart configurations using experimental information and some geometrical, topological and structural characteristics of the material. The simulation procedure is outlined in Section 4, which is then followed by a discussion of the results in Section 5.

2. Summary of earlier works

There has been a wealth of experimental information available from a range of studies including from Raman scattering, Electron and X-ray diffraction to Auger spectroscopy; however, none of these studies can provide a conclusive picture of the structural properties in the amorphous state. A number of experimental studies (such as Raman scattering [8] and X-ray diffraction [9]) have indicated significant presence of chemical disorder via homonuclear bond formation, whereas there are evidence from Auger [10], X-ray photoemission [11], and extended X-ray absorption [12] experiments indicating presence of heteronuclear bonds. Kaloyeros et al [12] performed extended X-ray absorption spectra and energy loss fine structure experiments to study sputtered a-SiC films and concluded that the short range chemical order was essentially consisting of only Si–C heteronuclear bonds. An X-ray adsorption and Raman spectroscopy study of SiC amorphized by ion bombardment by Bolse [13] concluded that the chemical short range order not only comprised of Si–C bonds but also homonuclear C–C and Si–Si bonds. Electron diffraction studies of SiC amorphized by ion beams confirms this observation [9], and shows the recovery of the SRO upon

annealing to 1073 K [14]. Fast neutron irradiation induced amorphization of SiC experiments by Snead *et al* revealed that the atomic density of *a*-SiC 2.85 g/cm^3 at 300 K increased to 3 g/cm^3 after annealing at 1100 K due to the recovery of SRO [15]. The picture that emerges from these experimental results points to the fact that *a*-SiC consists of both homo and heteronuclear bonds but it is difficult to quantify to what extent the short range chemical order is present in the network.

As far as theoretical studies are concerned, a fair amount of work can be found in literature [16, 17, 18, 19, 20, 21, 22, 23, 24, 25, 26, 27]. Finocchi and co-workers [16] were the first to perform a quench-from-the-melt *ab initio* molecular dynamics study using a 54- and 64-atom supercells and observed that 45% of the total bonds formed by C were homonuclear, of which 15% of the bonds were 3-fold coordinated (sp^2) with bond angles close to 120° (making these regions essentially graphite-like) and that *a*-SiC had negligible chemical ordering. A subsequent study by Kelires [17] via quench-from-the-melt Monte Carlo simulations of a 216-atom *a*-SiC sample using the empirical Tersoff potential [18] observed strong chemical ordering, but 50% of the C atoms were 3-fold coordinated and 33% of the C bonds were homonuclear. In an attempt to resolve the discrepancy, Tersoff [19] performed classical MD simulations using an improved version of the empirical potential [18] introducing a measure of chemical disorder via the ratio

$$\chi = \frac{n_{CC}}{n_{SiC}} \tag{1}$$

where n_{CC} is the number of C–C bonds and $n_{\mathrm{S}iC}$ is the number of Si–C bonds. χ=0 implies no chemical disorder and χ=1 indicates complete disorder in the network. Based on this definition, the author concluded that if the graphite-like regions in Ref. [16] were excluded then the combined results in Refs. [16], [17] and [19] corresponded to $0.5 \leq \chi \leq 0.6$. Mura and co-workers [20] performed classical MD simulations for *a*-Si$_x$C$_{1-x}$ alloys in the composition range $0.125 < x < 0.875$ using the modified Tersoff potential and a 512-atom supercell. For *a*-Si$_{0.5}$C$_{0.5}$ they obtained $\chi = 0.6$ and concluded that for high C contents, the value of χ is linked to a sizable distortion of the Si sublattice. Ivashchenko *et al* [21] performed sp^3s^* tight-binding MD simulations for models of *a*-SiC containing 54 to 216 atoms. They observed the existences of homonuclear bonds and coordination defect concentration of 6% to 13%. MD simulations of ion or neutron bombardment of *a*-SiC have been performed by Gao and Weber [22] and by Malerba and Perlado [23]. Gao and Weber [22] used the Tersoff potential [19] and obtained χ=0.41 in the damaged region created by 10 KeV Au recoils in a 250,000-atom supercell of 3C-SiC. Similarly, using classical MD simulations and a different version of the Tersoff potential [18], Malerba and Perlado [23] studied the damage accumulation process for 100 eV recoils in a 512-atom supercell of 3C-SiC embedded in a larger bounding crystal containing 1216 atoms. They obtained $\chi = 0.34$ for both the irradiated *a*-SiC and the reference quench-from-the-melt model of *a*-SiC. However, χ reduced to 0.22 in the irrdiated model and remained at 0.34 for the reference quench-from-the-melt model. Since previous simulations using the Tersoff potential [17, 19] produced χ=0.5–0.6, the rather different results (χ=0.22–0.34) by Malerba and Perlado [23] obtained using the same potential as described above is quite puzzling. However, Yuan and Hobbs have shown that if the amorphous-crystalline boundary is excluded, then the results of Malerba and Perlado [23] will correspond to (χ=0.35–0.5). Quite recently, Devanathan *et al* [25] have performed classical MD simulations using a Brenner-type interatomic potential [26] to model 4096-atom configuration of *a*-SiC. They observed that the density of the quenched

liquid was in excellent agreement with experiment and χ=0.06–0.13 for annealing temperatures ranging from 300 K to 2500 K. Finally, Rino *et al* [27], using an empirical potential with Coulomb, charge-dipole and Van der Waals interactions included in the two-body term, performed classical MD simulation for a large supercell of *a*-SiC containing 10,648 atoms and obtained χ=0, in perfect agreement with the experiments by Kaloyeros *et al* [12].

In summary, the bulk of the experimental and theoretical studies appear to favor a non-zero value of χ with the exception of the experimental work by Kaloyeros *et al* [12] and the theoretical models proposed by Rino *et al* [27]. As mentioned before, experimental results indicate that bonding in amorphous SiC is a mixture of both homonuclear and heteronuclear bonding consisting of sp^2 and sp^3 hybridizations. Given the complex nature of bonding chemistry in the amorphous environment, it is not surprising that models based on empirical or semi-empirical potentials are at best incomplete to describe some of the structural and electronic properties of *a*-SiC. Since most of the theoretical models proposed so far are based on either empirical or semi-empirical potentials, it is important to carry a full scale first-principles study of *a*-SiC so that the details of the quantum mechanical nature of the bonding between C and Si and the local chemistry can be taken into account in the model construction. While the models proposed by Finocchi *et al* [16] did take into account the quantum mechanical interactions within the density functional theory via local density approximation, the size of the simulation cell (typically 64 atoms) was too small to represent a realistic properties of bulk *a*-SiC. Since structural properties are directly linked with the electronic and vibrational properties of the materials, a predictive structural modeling should be done in conjunction with electronic and vibrational properties calculations for a reasonable system size, and to be compared with experiments. Finally, there are very few models in the literature that address the electronic properties of *a*-SiC [16, 21]. The present study attempts to provide a comprehensive picture of the structural and electronic properties of the alloy by selectively sampling the solution using the prior information obtained from experiments.

3. Strategy of our approximate simulation: sampling solution space with prior information

In conventional electronic structure problem one begins with a set of atomic coordinates and an interacting potential or Hamiltonian. The electronic density of states is obtained either by solving the Schrödinger equation within the first-principles density functional formalism or by constructing a semi-empirical Hamiltonian to compute the electronic eigenstates, total energy, and response functions to compare with experiments [28]. For amorphous materials, however, such an approach brings only a limited success. The determination of a ground state configuration (or an approximated one) of a glassy system involves identification of the global (or a low lying local) minimum in the multidimensional energy landscape, which is a very difficult problem in computational sciences. The complexity of the problem increases enormously with the increase of system size, and can be solved for a few simple potentials under strict mathematical conditions. The brute force applications of first-principles energy functional to model large amorphous systems is not only hopelessly difficult, but also uninspiring and time consuming. Most of the *ab initio* methods asymptotically scale as $O(n^3)$ or even faster that seriously constrain the size of the simulation cell and total time to be studied. The so-called order-N counterpart of such

approaches can improve the situation; however, for disordered materials the use of such methods are frankly very risky. The latter exploits the locality of quantum mechanics either via short-range nature of Wannier functions or truncation of density matrix of the system, but such requirements are rarely satisfied at the beginning of simulation for an arbitrary starting configuration. The prohibitive scaling constrains the system to evolve only for a limited time preventing it to explore the full solution space. Except for small system size and for few good glass formers, direct *ab initio* calculations tend to produce unrealistic configurations of the material, and the situation is particular exacerbated for (amorphous) materials that do not display glassy characters (e.g. amorphous silicon).

In recent years there have been a number of methods that make use of the available knowledge of the materials (either experimental or otherwise) in the simulation methodology. These 'knowledge-oriented' approaches have been developed under the general class of techniques based on information paradigm. Under this wing, one combines the power of first-principles force-field with the available information of the material under study. The general strategy is to construct a series of guesses of the solution that are consistent with experimental observation, and to improve the solution either deterministically or stochastically via an appropriate force-field. Examples of methods that are currently in use include 'Decorate-and-Relax' [29], 'Block-MD' [30] and 'Experimentally constrained molecular relaxation (ECMR)' [31], where prior knowledge of the materials are used to accelerate search procedure for finding a better minimum in the simulation methodology. Imposition of suitably constructed prior (information) reduces the volume of the search space by hierarchically constructing more probable solution space, and the system is driven to find the best solution in this subspace. Since the system spends most of its time in the favorable subspace of the desired solutions, it is computationally more efficient and it is likely to find a better estimate of the global minimum of the problem. The essential idea is to 'throwing out' the irrelevant part of the solution space by judicious choice of constraints and experimental data available for the material. While there exists no general scheme for guessing a series of candidate solutions for a complex multinary system, one can nonetheless construct a set of disordered networks that shares some of the characteristic features of the material (here *a*-SiC) obtained from experiments. This is done by introducing various priors in the network, which identify and sample the more probable part of the solution space associated with that priors.

Following this strategy, the starting point of our calculation is to build a series of binary random networks having some degree of local tetrahedral order. Each of the binary networks is then given different geometrical and topological character by changing the bond length, angles, coordination and different ring geometry. From a macroscopic point of view, all of these structure have almost identical tetrahedral character (of varying degree), but topologically they are quite different. A number of samples are generated with varying degree of chemical and topological disorder so that during the course of simulation the system has access to entire solution subspace of approximated tetrahedral ordering. The particular choice of ordering is motivated by the available experimental data from *a*-SiC (such as structure factor and bond angle distribution) suggesting presence of significant tetrahedral-like ordering in the material. It is to be noted that the topological character of this local ordering is very different from the randomized *c*-SiC structure [32], which is often used as a starting configuration without much care. While an unbiased, completely random configuration would be ideally the best choice to build the model during the course

of simulation, such a choice requires exploring a vast amount of solution space at the expense of computation time without the guarantee of identifying the correct minimum from the potentially correct solution set. The method can be made feasible for identifying the global minimum in small systems (such as clusters, macromolecules and some glasses) [33], but for large systems the number of solutions diverge rapidly with system size. In the present work, the binary random networks are generated via modified Wooten, Winer and Weaire (WWW) [34] algorithm as proposed by Barkema and Mousseau[35, 36]. The structural and topological properties of these binary networks are further modified so that the resulting networks span the subspace of the entire solution space that are consistent with available experimental data. In particular, we focus here on a 1000-atom model with 50-50 concentration of Si and C having the same density as that of experimental atomic density of crystalline 3C-SiC.

4. Molecular dynamics simulation procedure

In this work we have used the *ab initio* program SIESTA [37, 38, 39], which is capable of determining the electronic structure and properties of molecules, surfaces and bulk materials based on density functional theory (DFT). The Perdew-Zunger formulation of the local density approximation (LDA) is employed [40] along with the norm-conserving Troullier-Martins pseudopotentials [41] factorized in the Kleinman-Bylander form [42] to remove core electrons. To describe the valence electrons, a set of atomic orbitals basis are used consisting of finite-range numerical pseudoatomic wave functions of the form proposed by Sankey and Niklewski [43]. We employ a single-ζ (SZ) basis set on all atoms (one s and three p orbitals per atom) for the present calculation. Although some tight-binding calculations have indicated the need for an improved basis set beyond single-ζ, in this work we restrict ourselves to a single-ζ basis to minimize our computational effort. A real space mesh equivalent to a plane wave cut-off of 100 Ry is used for the evaluation of the Hartree and exchange-correlation energies. Owing to the large system size and the cubic scaling of the computational effort with system size, we implement the approximation by Harris [44], which is a non-self consistent version of DFT based on the linearization of the Kohn-Sham equations. The eigenvalue equations are solved by full diagonalization of the Hamiltonian matrix.

We performed a constant volume MD simulations using the Nosé thermostat with a time step Δt=1.0 fs. The simulation procedure consists of the following steps: (i) the temperature of the system is initially raised to 2500 K and is equilibrated for about 0.5 ps (ii) the resulting system is then cooled down to 1000 K over a time period of 1 ps in steps. (iii) We then equilibrate the system at 1000 K for 0.5 ps (iv) followed by cooling to 300 K over a time period of 1 ps. (v) The system is further equilibrated at 300 K for 0.5 ps, (v) and finally it is relaxed at 0 K to the nearest minimum using the conjugate gradient (CG) method until the maximum atomic force on each of the atoms is less than 0.03 eV/Å. These steps are then repeated for each of the candidate solutions mentioned in Section 3.

5. Results and discussions

5.1. Local structure and bonding environment

We begin our discussion by focusing on the local structure and the bonding environment of the atoms via 2- and 3-body correlation functions. The correlation
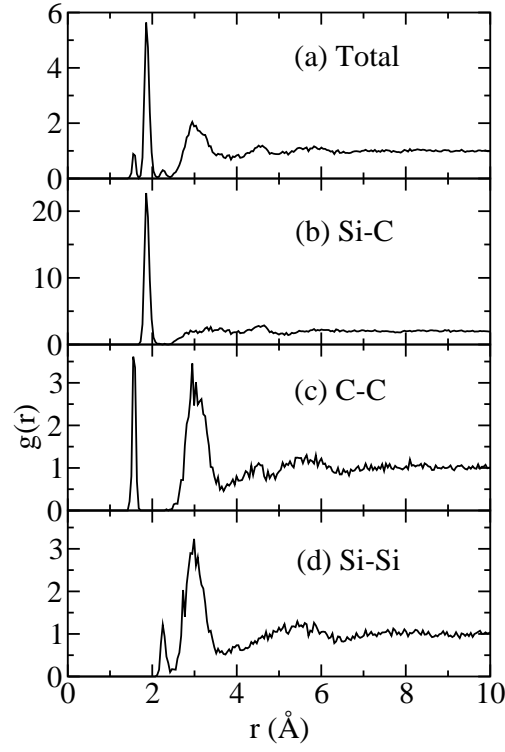
Figure 1. The total and partial radial distributions for the various pairs obtained from the model network. The distributions are all normalized for the purpose of comparison.
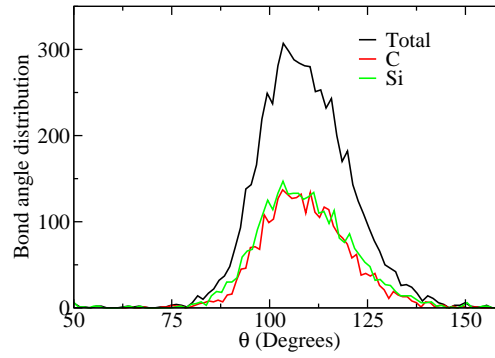

Figure 2. (Color online) The bond angle distributions for a-SiC network as discussed in the text. The distributions for angles centered at C and Si atoms are plotted along with the total bond angle distribution as indicated in the figure.

functions are calculated as radial and bond angle distributions providing information on the nature of short-range order in the network. For this binary system, we have studied three partial radial distributions of the components: C–C, Si–C and Si–Si. Together with the reduced 3-body correlation, the bond angle distribution, the local network properties can be studied and compared to the structural data from experiments. In figures 1(a)-(d), we present the normalized total and partial radial distribution functions (RDF). The Si-C first maximum peak in fig. 1(b) is clearly seen at around 1.9 Å, which is in agreement with experiments [12, 9] and previous theoretical calculations [16, 17, 19, 20, 21, 23, 24, 25, 27]. Similarly, the C–C and Si–Si first maxima at 1.55 Å and 2.25 Å respectively, are also in agreement with experimental data [9]. The total RDF in fig. 1(a) clearly indicates a dominant Si-C peak implying presence of strong chemical order in the network. A comparison of the peak heights of the C-Si and C-C from the partial RDFs suggests that the network is dominated by chemical order as far as the RDFs are concerned.

Further information about the local environment can be obtained via studying the coordination between Si and C atoms. For this purpose, we have used the location of the first minimum from the partial radial distributions as cut-off distances to define the first coordinations shells. In particular, the Si–C, C–C and Si–Si nearest neighbor cut-offs have been found to be R_{Si-C}=2.25 Å, R_{C-C}=1.9 Å and R_{Si-Si}=2.5 Å. The bond angles centered at Carbon and Silicon atoms are also calculated using the same cut-offs parameter. In fig.2, we plot the bond angle distributions for the C- and Si-centered angles along with the total bond angles. The average bond angle for the total distribution has been found to be $\langle\theta\rangle = 109°$ with a root mean square (RMS) deviation of about $\Delta\theta$=12.1°. The corresponding values for the partials are $\langle\theta\rangle_C$ = 109.2°, $\Delta\theta_C$=11.3° and $\langle\theta\rangle_{Si} = 108.7°$, $\Delta\theta_{Si}$=12.9°. This suggest that the final network continues to display tetrahedral character of its its crystalline counterpart. Together with the short range chemical order (manifested in the partial RDFs) and atomic coordination, the width of the bond angle distributions determine the overall quality of the network. A large value of the width $\Delta\theta$ is an indicative of high degree of disorder that affects the electronic properties by introducing gaps states in the electronic spectrum. Since electronic properties play an important role structure evaluation, a comparison with the other models in the literature would be relevant at this point. Devanathan *et al* [25] obtained a value of $\Delta\theta_C$=16° and $\Delta\theta_{Si}$=36°, whereas Rino *et al* [27] reported a value of $\Delta\theta_C$=15° and $\Delta\theta_{Si}$=16°.

A question of considerable importance and somewhat controversial is the extent of chemical disorder present in amorphous SiC network. Unlike amorphous silicon where sp^3 hybridization is the mechanism of bond formation between the neighboring atoms, the carbon chemistry permits C atoms to bond via sp^1, sp^2 and sp^3 hybridization making the local structure much more complex in disordered environment. Following Tersoff [19], we define a short range order parameter χ as the ratio of the number of C–C and C–Si bonds present in the network. Denoting n_{AB} (where A/B = Si, C) as the percentage of A–B bonding, we have found the values of C–C, Si–C, and Si–Si as 7.1%, 85.5%, and 7.4% respectively. Similarly, the percentage C_k of atoms that are k-fold coordinated have been found to be 2.6% (3-fold), 95.3% (4-fold), 2.0% (5-fold), and 0.1% (6-fold) respectively. This shows that the total coordination defect concentration is only about 4.7%, implying a minor deviation from an ideal 4-fold coordination. The percentage of C–C, Si–C and Si–Si bonds are respectively n_{CC}=7.1%, n_{SiC}=85.5% and n_{SiSi}=7.4%, giving χ of about χ=0.083. A comparison of the various structural parameters with earlier studies is presented in Table 1.

Table 1. Comparison of various structural parameters between this work and the previous experimental and theoretical works. $\langle N_C \rangle$ and $\langle N_{Si} \rangle$ are the partial average coordination numbers of C and Si respectively, while $\langle N \rangle$ is the total average coordination number. The chemical disorder parameter is denoted by $\chi = n_{CC}/n_{SiC}$, where n_{CC} and n_{SiC} are the percentage of C–C, Si–C bonds respectively.

	χ	$\langle N_C \rangle$	$\langle N_{Si} \rangle$	$\langle N \rangle$
Present work	0.083	3.98	4.01	4.00
Kaloyeros 1988[a]	0.00			3.99
Finocchi 1992[b]	0.6	3.85	3.93	3.89
Kelires 1992[b]	0.5	3.46	4.02	3.74
Tersoff 1994[b]	0.50	4.00		
Mura 1998[b]	0.60			
Ivashchenko 2002[b]*	0.027	3.94	3.96	3.95
Gao 2001[b]				
Rino 2004[b]	0.00			3.79

[a] Experiment
[b] Theory
* Configuration labelled TB-216D in Ref. [21].

Table 2. Irreducible ring statistics based on the nearest neigbbour cut-off defined in the text.

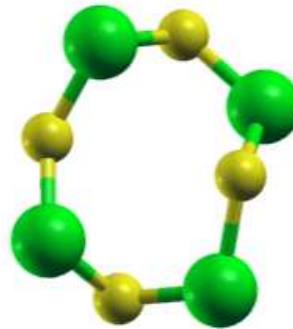| Ring size	3	4	5	6	7	8	9
Rings per atom	0.002	0.015	0.432	0.749	0.495	0.146	0.040

Figure 3. (Color online) A representative 6- and 8-member irreducible rings present in the network. The Carbon and Silicon atoms are shown in yellow (small) and green (large) respectively.
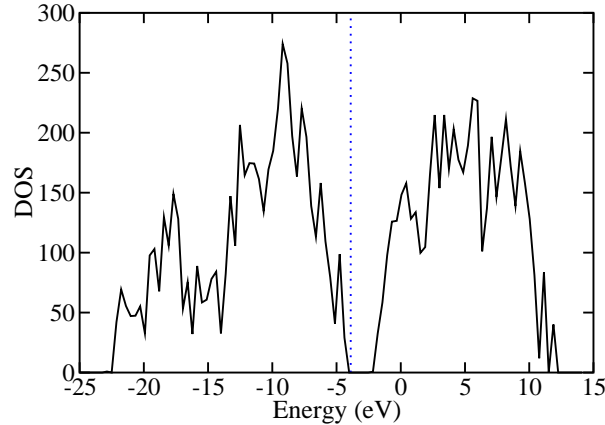
Figure 4. The electronic density of states for a-SiC network obtained from a first-principles Siesta Hamiltonian discussed in the text. The eigenvalues are broadened using a gaussian width of 0.01 eV. The Fermi level is indicated as a dashed vertical line in the figure.

In order to get the topological connectivity of the network, the type and the number of rings present are structure are computed. The irreducible ring statistics for various n-member rings are computed and the results are reported in Table 2. We define an irreducible ring as one such that it cannot be further partitioned into smaller rings. In other words, for a ring of size n, the minimum path starting from a given atom and to coming back to the same atom in an irreversible manner consists of n hops. A 6-member ring, which is the only ring in crystalline SiC (with ZnS structure), is dominant in our network followed by 7- and 5-member rings. This again implies the presence of tetrahedral character as already observed via bond angle distribution. Owing to few homonuclear bonds, almost all the rings consist of alternating Si and C atoms. In fig. 3, we have shown two representative 6- and 8-member rings.

We summarize the structural properties by noting that 1) the network has small RMS width of the bond angle deviations compared to models in the literature, and 2) having low coordination defect. Together with these, the ring statistics further confirms that the network is not strained and, therefore, should have good electronic properties. The latter aspect of the model is addressed in the next section in this paper. Furthermore, we have also noted, contrary to previous calculations [16, 17], no graphene-like structure (3-fold coordinated planer carbon region) with $\theta=120°$). This is not surprising in view of the fact that our model has a very few C-C wrong bonds.

5.2. Electronic Properties

While a great deal of information can be obtained from studying structural properties of the network via 2- and 3-body correlation functions and local coordination analysis, the electronic spectrum provides a more refined aspect of the local environment. In particular, the degree of local disorder is reflected in the local electronic density of states (l-EDOS) via formation of gap states and in the nature of the band tails of the spectrum. A high degree of local disorder causes the gap narrow and noisy, which is difficult to gauge from only partial RDFs and bond angle distribution. Partial

coordination number analysis does provide some information on the nature of eletronic density of states (e.g. presence of dangling bonds), but for a detailed understanding of eletronic properies and the nature of the wave functions near the band gap(s), one needs to calculate eletronic density of states of the model network. This is particularly important for models obatined via empirical potentials, but care must be taken into account to make sure the electronic density of states is reasonably good, and reflects the correct local chemistry. The electronic density states for our model is obtained via diagonalization of the density functional Hamiltonian from SIESTA.

In fig. 4, we have presented the gaussian-broadened electronic density of states (EDOS) for the single particle Kohn-Sham energy eigenvalues. Several important observations are in order. First, the model shows the presence of a clean spectral gap. For a finite system, the gap size can be estimated as the difference between the highest occupied molecular orbital (HOMO) and the lowest unoccupied molecular orbital (LUMO). The exact value of HOMO-LUMO gap for our model is found to be 1 eV, which is about 1.2 eV smaller than the experimental bandgap for 3C-SiC of 2.2 eV [45]. However, as observed from the fig. 4, the average gap size is greater than 1 eV and is much closer to the experimental value taking into account some defect states that are close towards the main conduction band. It is noteworthy that even though LDA underestimates the size of the gap, our model does produce the presence of almost clean gap in the spectrum. This is a further indication that our method correctly identifies low lying minima in the configuration space. We want to emphasize that this is an important aspect of our method despite being approximate in nature.

A further characterization of our model comes from the nature of the band tail states. In an amorphous system, one expects the band tail states to show some signature of localization due to topological and chemical disorder in the network. This is independent of the presence of defect in the system. To study this, one often uses an *ad hoc* measure for eigenstate localization known as the *inverse participation ratio* (IPR). In a simplest way, IPR approximately measures the *reciprocal* of the number of atoms that participate in localizing an eigenstate. While IPR is not the best way to quantify degree of localization, it does provide some qualitative idea about the spread of an eigenstate over the atoms. For a multi-band Hamiltonian, given a normalized eigenstate ψ with eigenenergy E, we first compute the Mulliken charge contribution from each atom q_i by projecting the eigenvector onto the orbitals centred on atom i and then sum over the orbitals to get the total contribution. The IPR can be expressed as,

$$\text{IPR}(E) = \sum_{i=1}^{N} q_i^2 \tag{2}$$

where N is the total number of atoms. If the eigenstate ψ is completely localized, then only a single atom participates in localizing ψ, yielding IPR(E)=1. Otherwise, if ψ is completely delocalized, then all atoms participate in localizing ψ, giving IPR(E)=1/N. Thus large values of IPR generally correspond to localized states and vice versa. In fig. 5, we plot the electronic IPR versus energy eigenvalue in the vicinity of the Fermi level. Each spike is located at an energy eigenvalue. The values of the IPR clearly show that the states near the band gap are more localized than of the states away from the gap. A pictorial representation often helps better to understand this behavior and is presented in fig. 6. To this end, we assign different colors to each site according to its Mulliken charge contribution for a given eigenstate. We then depict
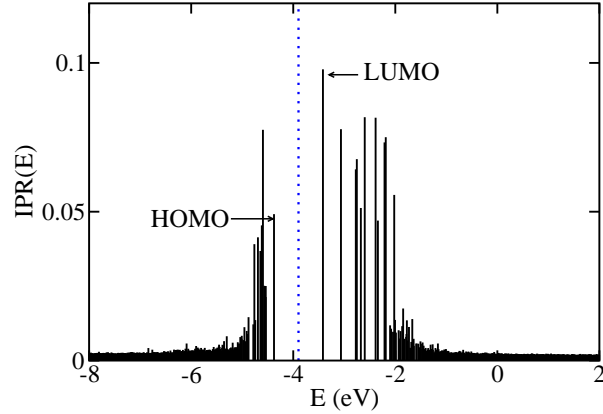
Figure 5. Inverse participation ratio (IPR) for the 1000-atom a-SiC model as a function of electronic eigenvalues. The highest occupied (HUMO) and the lowest unoccupied molecular orbitals are shown in the figure. The large IPR values reflect the localized nature of the states in real space.
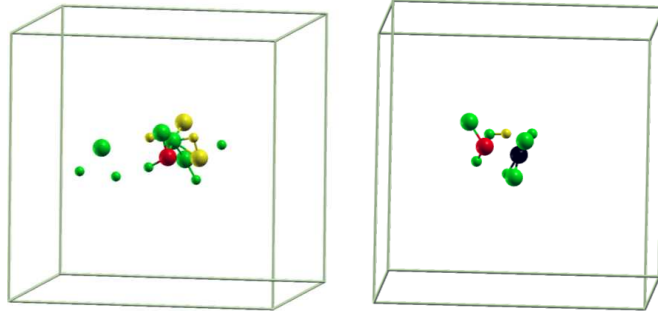
HOMO E=-4.38 eV IPR=0.05 LUMO E=-3.42 eV IPR=0.098

Figure 6. (Color online) Spatial character of the localized HOMO (left) and LUMO (right) eigenstates. Silicon atoms are shown somewhat larger than the C atoms. The following color code is used to map the Mulliken charge q for the states at each atomic site: black ($q > 0.20$), red ($0.10 < q \leq 0.20$), gold ($0.05 < q \leq 0.10$) and green ($0.01 < q \leq 0.05$).

the spatial feature by showing a fraction (70%) of the total charge for the HOMO and LUMO states in the plot.

It is clear from the fig. 6 that the eigenfunctions (corresponding to HUMO and LUMO) mostly confined to a small cluster of atoms in space. While the size of the cluster is, to an extent, dependent on the chosen fraction of Mulliken charge, it's nonetheless confirms that the localized nature of the states in real space. For the occupied state, a silicon atom (large and colored red in the plot) has the largest contribution of about 14% of the unit charge. The atom is 4-fold coordinated, and have 2 homonuclear and 2 heteronuclear bonds. For the LUMO state, the largest contribution to the Mulliken charge is about 25% from a silicon atom (colored black). The atom is also 4-fold coordinated with 2 homonuclear and 2 heteronuclear bonds.

5.3. Vibrational Spectrum

The vibrational density of states (v-DOS) of the model can been studied by computing the vibrational eigenmodes and eigenfrequencies. Since the energy associated with a typical vibrational degree of freedom is much lower than that of the eletronic, a slight deviation in the local geometry can cause a significant deviation in the vibrational spectrum and the modes of the vibration of the atoms. Such changes often can be difficult to observe in electronic density of states, and therefore, for a full characterization of the model one need to ascertain the vibrational eigenmodes and the nature of vibrations. In this work, we address this issue by computing the modes via direct diagonalization of the dynamical matrix. Once the eigenmodes are available, the corresponding vibrational IPR can be calculated for each of the eigenfrequencies and the nature of the modes can be studied.

The dynamical matrix elements are constructed by successively displacing each atom in the fully optimized supercell along the positive and negative direction of the three orthogonal axes, and computing the resulting atomic forces within the harmonic approximation. Unlike the electronic IPR, we define here the vibrational IPR in a somewhat different way. Denoting a normalized vibrational eigenmode with frequency ω by $\boldsymbol{\Phi} = (\boldsymbol{\Phi}^1, \boldsymbol{\Phi}^2, \ldots, \boldsymbol{\Phi}^N)$, where $\boldsymbol{\Phi}^i = (\Phi_x^i, \Phi_y^i, \Phi_z^i)$ and i is the atomic index, the IPR is defined as

$$\mathrm{IPR}(\omega) = \sum_{i=1}^{N} (\boldsymbol{\Phi}^i \cdot \boldsymbol{\Phi}^i)^2 \tag{3}$$

For an ideally localized $\boldsymbol{\Phi}$, only one atom contributes to the vibrational amplitude and so IPR(ω)=1. Similarly, for an ideally delocalized $\boldsymbol{\Phi}$, all atoms contribute uniformly to the amplitude yielding IPR(ω)=1/N.

In fig. 7 we show, in the upper panel, the plots for the atom-projected (weighted by the atomic contribution to the amplitude of the eigenstate conjugate to a given eigenfrequency) and total v-DOS. The corresponding vibrational IPR is plotted in the lower panel. The v-DOS clearly shows that the low frequency bands are dominated by Si while the high frequency bands are dominated by C. The overall shape and peak positions of the partial and the total v-DOS are in agreement with recent calculations by Vashishta *et al* [7] using an empirical potential. The IPR for the vibrational modes clearly distinguish two different type of modes: low frequency extended modes primarily arising from the Si atoms and the high frequency localized modes originate mostly from the C atoms. The nature of the vibrational mode can be obtained by studying the corresponding eigenmode and the contribution from each of the atoms. The most localized vibrational mode appears at frequency 142 meV having IPR value 0.634. A real space analysis reveals that the vibration corresponds to this mode is a Si–C stretching mode with 78% of the mode confined on the C atom, and about 12% on the Si atom leaving behind the rest 10% on the neighboring atoms. Similar analysis of the other localized states suggest all the high frequency states are localized and are centered on C atoms.

6. Conclusion

We present an approximate first-principles molecular dynamics simulation of *a*-SiC within the density functional formalism coupled with a priori information obtained from experimental data. The method consists of generating a set of smart structural
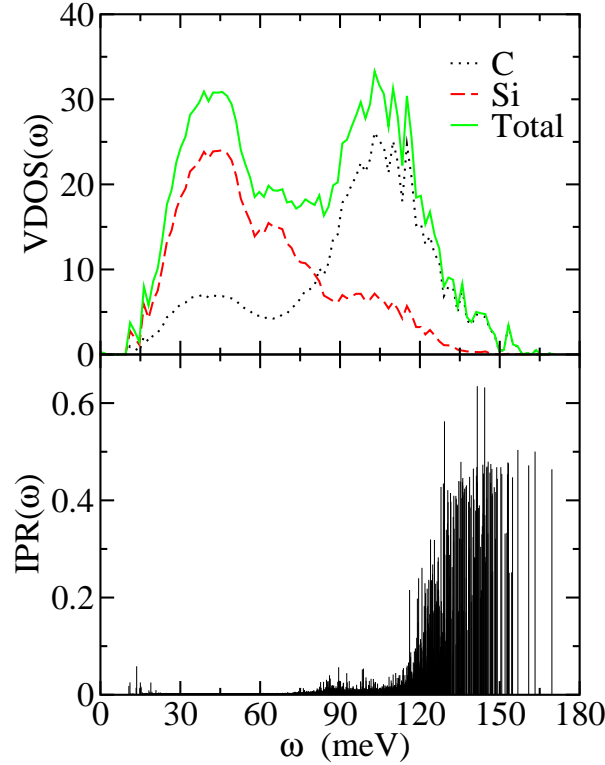
Figure 7. (Color online upper panel) Atom-projected and total vibrational density of states (upper panel) and vibrational IPR (lower panel) for the 1000-atom *a*-SiC model. The majority of the high frequency vibrational modes are localized around C atoms of C–C and Si–C bonds.

configurations as candidate solutions starting from a generic binary tethedral network and importance sampling the configuration subspace by incorporating characteristic structural, topological, and experimental information. Each of the samples is then used in our *ab initio* constant temperature molecular dynamics to find the minimum energy configuration, and the global minimum of this set used as a final solution in our work. We have studied structural, electronic and vibrational properties for 50-50 *a*-SiC by using a localized basis first-principles molecular dynamics method. The degree of chemical disorder, expressed as a ratio of the C–C to the Si–C bonds is found to be approximately 0.083. The percentage of C–C, Si–C and Si–Si bonds in the network are observed to be 7.1%, 85.5% and 7.4% respectively. The coordination defect concentration found in our model is low and is about 4.7%, while the average bond angle and its RMS width are about 109° and 12.1° respectively. The electronic spectrum reveals a reasonably clean gap (HOMO-LUMO) of size about 1 eV taking into account the defects states in the gap. Inverse participation ratio (IPR) analysis indicates that the electronic band tail states are fairly localized with almost central atom being 4-fold coordinated, and having at least one wrong bond. Similar analysis of the vibrational spectrum within the harmonic approximation suggests that the low frequency bands are dominated by Si vibrations whereas the C atoms mostly involve

with the high frequency vibrational modes. A real space analysis of the high frequency vibrational modes (identified via IPR) shows that the vibrations are mostly stretching in character with larger contribution coming from the C atoms.

Acknowledgments

[1] Levinshteæin M E, Rumyantsev S L and Shur M 2001 *Properties of Advanced Semiconductor Materials: GaN, AlN, InN, BN, SiC, SiGe* (New York: Wiley)
[2] Emin D, Aselage T L and Wood C (eds) 1987 *Novel Refractory Semiconductors* Vol **97** of the Materials Research Society Symposium Proceedings (Materials Research Society, Pittsburgh, USA)
[3] Marshall R C, Faust J W and Ryan C E, *Silicon Carbide-1973; Proceedings* Air Force Cambridge Research Laboratories (U.S.) and University of South Carolina 1st edn 1974 (Columbia: University of South Carolina Press)
[4] O'Connor J R and Smiltens 1960 *Silicon Carbide, A High Temperature Semiconductor; Proccedings* Air Force Cambridge Research Laboratories (U.S.) Electronic Research Directorate (Oxford: Pergamon)
[5] Pechenik A, Kalia R K and Vashishta P 1999 *Computer-aided Design of High-Temperature Materials* (New York: Oxford University Press)
[6] Thorpe M F and Mitkova M I (Editors) 1997 *Amorphous Insulators and Semiconductors* North Atlantic Scientific Affairs Division (Dordrecht: Kluwer Academic)
[7] Vashishta P, Kalia R K and Nakano A 2007 *J. Appl. Phys.* **101** 103515
[8] Gorman M and Solin S.A 1974 Solid State commun. **15** 761
[9] Ishimaru M, Bae I-T, Hirata A, Hirotsu Y, Valdex J A and Sickafu K E 2005 *Phys. Rev.* B **72** 024116
[10] Lee W.Y 1980 *J. Appl. Phys.* **51** 3365
[11] Katayama Y, Usami K and Shimada T 1981 Philos. Mag B **43** 283
[12] Kaloyeros A E, Rizk R B and Woodhouse J B 1988 *Phys. Rev.* B **78** 13099
[13] Bolse W 1999 *Nucl. Instrum. Methods* B **148** 83
[14] Ishimaru M, Bae I-T, Hirotsu Y Matsumura S and Sickafu K E, 2002 *Phys. Rev. Lett.* **89** 05502
[15] Snead L L and Zinkle S J 2002 *Nucl. Instrum. Methods* B **191** 497
[16] Finocchi F, Gali G, Parinello M and Bertoni C M 1992 *Phys. Rev. Lett.* **68** 3044
[17] Kelires P C 1992 *Phys. Rev.* B **46** 10048
[18] Tersoff J 1989 *Phys. Rev.* B **39** 5556
[19] Tersoff J 1994 *Phys. Rev.* B **49** 16349
[20] Mura D, Colombo L, Bertoncini R and Mula G 1998 *Phys. Rev.* B **58** 10357
[21] Ivashchenko V I, Turch P E A, Shevchenko V I, Ivashchenko L A and Rusakov G V 2002 *Phys. Rev.* B **66** 195201
[22] Gao F and Weber W J 2001 *J. Appl. Phys.* **89** 4275
[23] Malerba L and Perlado J M 2001 *Jour. Nucl. Mater.* **289** 57
[24] Yuan X and Hobbs L W 2002 *Nucl. Instrum. Methods* B **191** 74
[25] Devanathan R, Gao F and Weber W J 2007 *Nucl. Instrum. Methods* **255** 130
[26] Gao F and Weber W J 2002 *Nucl. Instrum. Methods* B **191** 504
[27] Rino J P, Ebbsjö I, Branicio P S, Kalia R K, Nakano A, Shimojo F and P Vashishta 2004 *Phys. Rev.* B **70** 045207
[28] Richard Martin, *Electronic Structure: Basic theory and practical methods* (Cambridge University Press 2004)
[29] Tafen D N and Drabold D A 2003 *Phys. Rev.* B **68** 165208
[30] Tafen D N and Drabold D A 2005 *Phys. Rev.* B **71** 054206
[31] Biswas P, Tafen D N and Drabold D A 2005 *Phys. Rev.* B **71** 054204
[32] Computer simulation of *a*-SiC starting with randomized diamond structure via the WWW bond switching algorithm (Ref. [34]) has indicated that for a small of degree disorder, the system

has the tendency to get back to the crystalline structure after relaxation. This is avoided by making bond switches beyond a critial number in WWW method, and by melting the initial structure in 'quench-from-the-melt' approach. A choice of randomized c-SiC as a starting structure may therefore be an inappropriate one unless the crystalline memory of the structure is fully eliminated.

[33] David Wales, *Energy Landscapes: Applications to Clusters, Biomolecules and Glasses* (Cambridge University Press 2003, Cambridge, UK)
[34] Wooten F, Winer K and Weaire D 1985 *Phys. Rev. Lett.* **54** 1392
[35] Barkema G T and Mousseau N 2000 *Phys. Rev.* B **62** 4985
[36] Mousseau N and Barkema G T 2004 *J. Phys.: Condens. Matter* **16** S5183
[37] Ordejón P, Artacho E and Soler J M 1996 *Phys. Rev.* B **53** 10441
[38] Sánchez-Portal D, Ordejón P, Artacho E and Soler J M 1997 *Int. J. Quantum Chem.* **65** 453
[39] Soler J M, Artacho E, Gale J D, Garcá A, Junquera J, Ordejón P and Sánchez-Portal D 2002 *J. Phys.: Condens. Matter* **14** 2745
[40] Perdew J Pand Zunger A 1981 *Phys. Rev.* B **23** 5048
[41] Troullier N and Martins J L 1993 *Phys. Rev.* B **43** 1993
[42] Kleinman L and Bylander D M 1982 *Phys. Rev. Lett.* **48** 1425
[43] Sankey O F and Niklewski D J 1989 *Phys. Rev.* B **40** 3979
[44] Harris J 1985 *Phys. Rev.* B **31** 1770
[45] See, for example, the review article by Morkoc H, Strite S, Gao G B, Lin M E, Sverdlov B and Burns M 1994 *J. Appl. Phys.* **76** 1363